HHS Public Access

Author manuscript

Mol Pharm. Author manuscript; available in PMC 2023 June 26.

Published in final edited form as:

Mol Pharm. 2021 February 01; 18(2): 714–725. doi:10.1021/acs.molpharmaceut.0c00461.

Design and Validation of Liposomal ApoE2 Gene Delivery System to Evade Blood–Brain Barrier for Effective Treatment of Alzheimer's Disease

Sanjay Arora,

Buddhadev Layek,

Jagdish Singh

Department of Pharmaceutical Sciences, School of Pharmacy, College of Health Professions, North Dakota State University, Fargo 58105, North Dakota, United States

Abstract

Targeting gene-based therapeutics to the brain is a strategy actively sought to treat Alzheimer's disease (AD). Recent findings discovered the role of apolipoprotein E (ApoE) isoforms in the clearance of toxic amyloid beta proteins from the brain. ApoE2 isoform is beneficial for preventing AD development, whereas ApoE4 is a major contributing factor to the disease. In this paper, we demonstrated efficient brain-targeted delivery of ApoE2 encoding plasmid DNA (pApoE2) using glucose transporter-1 (glut-1) targeted liposomes. Liposomes were surface-functionalized with a glut-1 targeting ligand mannose (MAN) and a cell-penetrating peptide (CPP) to enhance brain-targeting and cellular internalization, respectively. Among various CPPs, rabies virus glycoprotein peptide (RVG) or penetratin (Pen) was selected as a cell-penetration enhancer. Dual (RVGMAN and PenMAN)-functionalized liposomes were cytocompatible at 100 nM phospholipid concentration and demonstrated significantly higher expression of ApoE2 in bEnd.3 cells, primary neurons, and astrocytes compared to monofunctionalized and unmodified (plain) liposomes. Dual-modified liposomes also showed ~2 times higher protein expression than other formulation controls in neurons cultured below the *in vitro* BBB model. These results translated well to *in vivo* efficacy study with significantly higher transfection of pApoE2 in the C57BL/6 mice brain following single tail vein administration of RVGMAN and PenMAN functionalized liposomes without any noticeable signs of toxicity. These results illustrate the potential of surface-modified liposomes for safe and brain-targeted delivery of the pApoE2 gene for effective AD therapy.

Graphical Abstract

Corresponding Author: Jagdish Singh – Department of Pharmaceutical Sciences, School of Pharmacy, College of Health Professions, North Dakota State University, Fargo 58105, North Dakota, United States; Phone: +1-701-231-7943; jagdish.singh@ndsu.edu; Fax: +1-701-231-8333.

The authors declare no competing financial interest.

ASSOCIATED CONTENT

Supporting Information

The Supporting Information is available free of charge at https://pubs.acs.org/doi/10.1021/acs.molpharmaceut.0c00461.

Plasmid used in this work (PDF)

Complete contact information is available at: https://pubs.acs.org/10.1021/acs.molpharmaceut.0c00461

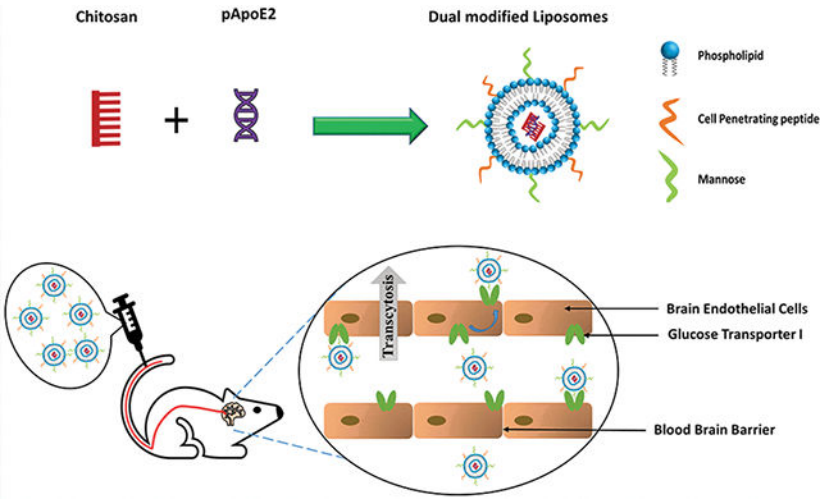

Keywords

Apolipoprotein; liposomes; glucose transporter; Alzheimer's disease; cell penetrating peptides

INTRODUCTION

The most common form of dementing illness of the central nervous system (CNS), which affects millions of people above the age of 65 around the globe, is Alzheimer's disease (AD).[1] AD is classified as an irreversible chronic neurodegenerative disorder associated with an enormous economic burden. It is estimated that by 2050, AD will afflict more than a million individuals each year in the USA alone.[1] Although AD was discovered more than 100 years ago, currently approved drugs can only provide symptomatic treatment, and no preventive or long-term solution is currently available.[2] In the last few decades, numerous biochemical hallmarks were discovered in AD patients like intracellular neurofibrillary tangles (NFTs) resulting from hyperphosphorylation of tau protein and extracellular amyloid-β (Aβ) plaque deposition.[3,4] Increased levels of Aβ protein have been linked with familial as well as sporadic AD, indicating a decline in its concentration may be advantageous.[5] Mounting experimental evidence supports the role of apolipoprotein E (ApoE) as a key element linked to Aβ levels as well as the amyloid burden in the brain during AD progression.[6–8]

ApoE is the primary apolipoprotein synthesized by brain astrocytes. It plays a crucial role in the transportation and distribution of cholesterol as well as synaptogenesis inside the brain.[9] There are three ApoE isoforms, namely, E2, E3, and E4, each predominantly expressed by brain and liver.[10] These isoforms differ from one another at 112 and 158 positions in their protein structure.[11] Inheritance of ApoE4 is regarded as one of the key factors correlated with the AD progression.[12] In comparison to ApoE3, ApoE4 homozygotes bear relatively greater risk (14.5 times) for AD development.[13,14] On the other hand, the E2 allele is protective in nature and reduces AD risk by 50% and also delays the onset of disease.[15,16] Experimental evidence shows that ApoE isoforms are chief elements influencing concentration and quality of Aβ peptide as well as Aβ burden in the brain

that accumulates during aging.[6] Clearance of Aβ peptide is differentially regulated by ApoE isoforms inside the brain.[17] In AD mice, the E4 isoform was found to be least effective in clearing brain Aβ, whereas E2 showed significantly improved clearance.[17] This can be attributed to the weak binding affinity of ApoE4 toward Aβ compared to other isoforms, resulting in isoform dependent clearance (E2 > E3 > E4) through neurons and microglia.[18–20] Presence of ApoE4 isoform is also shown to negatively affect dendritic length, density, and cognitive performance compared to E2 isoform.[21] Moreover, during aging, ApoE levels were found to be reduced in the hypothalamus and cortex, which may further attenuate the clearance of toxic Aβ proteins.[22] Based on these observations, in situ expression of ApoE2 isoform in brain tissue can be of significant therapeutic advantage to treat AD. However, the protective function of the blood–brain barrier (BBB) poses a major hurdle for effective gene delivery to the brain.[23,24] Although, viral vectors have shown promising results *in vitro*, their utilization is afflicted with life threatening adverse effects, including mutations, inflammatory reactions, and formation of toxins.[25,26]

In our present study, plasmid encoding ApoE2 (pApoE2) was delivered using liposomes. Liposomal nanoparticles have numerous advantages over their viral counterparts like high packing capacity, easy scale-up, reproducibility, and low immunogenicity, allowing safe and effective gene therapy.[27] Prior to incorporation, plasmid DNA was complexed to chitosan to facilitate DNA condensation and protect it from endolysosomal degradation.[28–31] Since, the luminal side of the BBB possesses glucose transporter-1 (glut-1)in high density; thus glut-1 substrate mannose (MAN) was used in the development of these nanoparticles.[32,33] Additionally, penetratin (Pen), a short chain cationic peptide, or a nicotinic acetylcholine receptor substrate, rabies virus glycoprotein peptide (RVG), were used along with MAN to enhance liposome transport to the brain. These cell-penetrating peptides (CPPs) lead to enhanced translocation through the BBB via acetylcholine receptor mediated transcytosis for RVG and direct transportation for Pen.[34–37] Monumental evidence suggests that nanoparticles modified using brain targeted ligands in combination with RVG have resulted in very promising brain targeting to treat cancer, AD, and Parkinson's disease.[28,38–40] Based on this evidence, RVG was chosen to be evaluated in combination with mannose for brain targeting. The rationale for using Pen was that previous in vivo studies from our group and other researchers have shown very promising results with this CPP for brain-targeted delivery of nanoparticles, pDNA, and antibodies.[40–43] Moreover, a comprehensive study evaluating the biodistribution of various CPPs used to target brain have shown Pen as the most favorable for delivery of cargoes to the brain.[44]

In our recent publication, we have demonstrated the efficacy of dual-functionalized liposomes for brain-targeted delivery of brain-derived neurotrophic factor (BDNF) plasmid DNA and its subsequent expression in the brain tissue.[40] However, due to the difference in size, half-life, and biochemical properties of expressed proteins, in our present study, we have explored the gene transfection efficiency of pApoE2 utilizing different liposomal formulations.[45,46] We have also elucidated the detailed mechanism of cellular internalization of these liposomes in the presence of various specific pharmacological endocytosis inhibitors. One of the significant challenges of ligand-mediated targeting is the intense competition from the physiological substrates, which often leads to functionality loss of the delivery system. Thus, the cellular internalization capacity of dual-functionalized liposomes

was further assessed in the presence of different glut-1 substrates at physiologically relevant levels. Lastly, the biocompatibility of the pApoE2-loaded liposomes was evaluated to determine the effect of cationic lipids and the expressed protein on brain cells *in vitro* and various organs.

MATERIALS AND METHODS

Materials.

Dioleoyl-3-trimethylammonium-propane chloride (DOTAP), dioleoyl-sn-glycero-3-phosphoethanolamine (DOPE), and lissamine rhodamine were purchased form Avanti Polar Lipids (Birmingham, AL, USA). DSPE–PEG2000–Mannose and DSPE–PEG2000–NHS were procured from Biochempeg Scientific Inc. (Watertown, MA, USA). Chitosan with a molar mass of 30 kDa was obtained from Glentham Life Sciences (Corsham, UK). Cholesterol, Hoechst 33342, ethylenediaminetetraacetic acid (EDTA), 4-(2-hydroxyethyl)-1-piperazineethanesulfonic acid (HEPES), and Triton X-100 were procured from Sigma-Aldrich (St. Louis, MO, USA). Phosphate buffered saline (PBS), fetal bovine serum (FBS), and Dulbecco's modified Eagle medium (DMEM) were acquired from Corning Incorporated (Corning, NY, USA). RVG (YTIWMPENPRPGTPCDIFTNSRGKRASNG) and penetratin (RQIKIWFQNRRMKWKKGG) were purchased from Zhejiang Ontores Biotechnologies Co., Ltd. (Zhejiang, China).

Preparation of CPP Conjugated DSPE-PEG2000.

Conjugation of CPP to DSPE-PEG2000-NHS was performed at a molar ratio 3:1 (lipid/peptide) as described previously.[47] Dimethylformamide (DMF) was used to dissolve the reactants, and the solution was alkalified (pH to 8.5) with triethylamine to facilitate this nucleophilic substitution reaction. The reaction was continued for 3 days under constant stirring followed by dialysis (MWCO 3.5 kDa) for 2 days against deionized water to remove unreacted CPPs and PEGylated lipids. The dialyzed product was lyophilized and micro-bicinchoninic acid (BCA) assay was conducted to measure the extent of CPP conjugation to DSPE-PEG. Finally, peptide bound lipid product was used to synthesize liposomes.[40,47]

Synthesis and Evaluation of Liposome Formulations.

Film hydration technique was used to prepare liposomes using DOPE, cationic lipid DOTAP, CPP conjugated PEGylated DSPE, MAN conjugated PEGylated DSPE, and cholesterol in 45:45:4:4:2 molar ratio. The methanol and chloroform solution (1:2) was used to solubilize lipids, and a uniform lipid film was produced using a rotary evaporator. Chitosan and ApoE2 pDNA were complexed (N/P 5:1) via electrostatic interactions and added to the hydration buffer (10 mM HEPES, pH 7.4). The liposomal dispersion was sonicated in a bath solicitor for 0.5 h, which resulted in the formation of small unilamellar vesicles. Dynamic light scattering (DLS) was utilized to measure size and surface charge at 25 °C. The percent entrapment of pApoE2 was determined using Hoechst 33342 fluorescent dye.[47,48]

Atomic force microscopy (DI-300 Veeco, MN, U.S.A.) was used to elucidate the surface morphology of liposomes. Liposome dispersion (4 μL) was dried on newly sliced mica using

nitrogen flow to form a thin layer. The film was scanned at a rate of 1 Hz using a pyramidal cantilever.

DNase Protection Assay.

Shielding of encapsulated ApoE2 plasmid from DNase I digestion was assessed by gel electrophoresis.[47] In brief, 1 μg of liposome entrapped chitosan/pApoE2 complex was incubated with DNase I enzyme (1 unit) for an hour at 37 °C. Naked plasmid was also incubated with the enzyme as positive control. Five microliters of EDTA solution (100 mM) was utilized postincubation to inactivate the DNase enzyme. Subsequently, the inactivated mixture was incubated with heparin (30 μL, 5 mg/mL) solution for 2 h to release pApoE2. Agarose gel electrophoresis was performed on the resulting mixture to assess the stability of released plasmid DNA at 80 V for 1.5 h.[47]

Cell Culture.

Primary rat astrocytes, bEnd.3 cells, and primary rat neurons were used to perform *in vitro* studies. bEnd.3 cells were procured from American Type Culture Collection (ATCC) and used up to 5 passages. Primary astrocytes and bEnd.3 cells were cultured in complete DMEM media (90% DMEM, 10% FBS, 1% PSF). Primary astrocytes and neurons were obtained from 1-day old Sprague–Dawley rat pup brains. A single cell suspension of brain tissue was obtained using an optimized protocol as described previously.[49,50] Primary neurons were cultured following a similar procedure using DMEM containing equine serum (10% v/v) and PSF (1% v/v). Additionally, cytosine arabinoside or AraC (10 μM) was included in culture media on day 3 and was changed with new medium without AraC on day 5. Anti-glial fibrillary acidic protein (GFAP) antibody was used to determine phenotype of cultured primary astrocytes and anti-MAP2 antibody for primary neuronal cells.

In Vitro Cytotoxicity Assay.

The cytocompatibility of liposomes was evaluated using bEnd.3 cells, primary astrocytes, and primary neurons.[51–53] Cells (5×10^3/well) were cultured in 96-well plates for 24 h, and pApoE2 containing liposomal formulations at various concentrations (50–600 nM total lipids in DMEM basal medium) were incubated with cells for 4 h. Subsequently, cells were washed, and fresh media was added and incubated further for 2 days. Postincubation, MTT (3-(4,5-dimethylthiazol-2-yl)-2,5-diphenyltetrazolium bromide) was added to the cell culture, and viability was estimated and compared to untreated cells.

Cellular Mechanism of Uptake and Competition Assay.

The detailed mechanism of nanoparticle uptake was elucidated in bEnd.3 cells. After plating (24 h, 5×10^4 cells per well), endocytosis inhibitors were added to the cell culture individually 30 min prior to liposomal treatment. Treatment at cold temperature (4 °C) or with 10 mM sodium azide impedes all ATP-dependent internalization pathways. Clathrin-mediated endocytosis and caveaolae formation by polymerization of microtubules were blocked using 10 μg/mL chlorpromazine and 100 μg/mL colchicine, respectively. Amiloride (50 μg/mL) was added to prevent internalization via micropinocytosis. After treatment with the various inhibitors, lissamine rhodamine labeled liposomes were added to culture media

containing each inhibitor and incubated for 1 h. Thereafter, PBS was used to wash cells, and cells were lysed using triton X-100. The lissamine rhodamine intensity was measured (λ_{ex} 553 nm, λ_{em} 570 nm) after extraction with methanol from cell lysates.[54]

A competitive inhibition experiment was carried out in bEnd.3 cells using different liposomal formulations. Cells were pretreated for 0.5 h with different strengths of D-glucose and D-mannose in PBS prior to the competition assay. Subsequently, lissamine rhodamine labeled liposomes were introduced to the cells and incubated for 1 h.[55] Postincubation, the liposomes internalization was evaluated as described earlier by measuring lissamine rhodamine concentration.

In Vitro Transfection Efficiency.

The studies were performed in 24-well plates (1×10^5 cells/well) using bEnd.3, primary astrocytes, and neurons. ApoE2 pDNA (1 μg) loaded in different surface-functionalized liposomes was used to treat cells in DMEM basal medium. Following 4 h of treatment, formulation containing media was replaced with complete media, and cells were incubated for 2 more days. ApoE ELISA kit (Thermo Fisher Scientific) was used to measure ApoE2 protein expression in cell lysates and supernatant media. Total protein was also quantified to normalize ApoE2 transfection. Transfection efficacy of liposomes was compared against the commercial transfection agent Lipofectamine 3000.

Development of BBB Model.

Preparation of the *in vitro* BBB model was done using primary astrocytes and bEnd.3 cells as previously reported.[56,57] Primary astrocytes ($1.5 \times 10^4/cm^2$) were cultured on the abluminal side of the culture insert, whereas bEnd.3 cells ($1.5 \times 10^6/cm^2$) were cultured on the top layer using 20% serum containing media to form the *in vitro* BBB. Epithelial Volt/Ohm Meter 2 (EVOM) was used to determine transendothelial electrical resistance (TEER) to establish barrier integrity. Flux of the BBB impermeable dye sodium–fluorescein (Na–F) was used to estimate paracellular transport across the coculture model.[58,59] This coculture and bEnd.3 cells monolayer models were moved to different wells containing 500 μL of PBS. Na–F in PBS (10 μg/mL) was added to each culture insert, and its transport was evaluated at various time points up to 1 h. The fluorescence intensity of Na–F in the culture insert and 24-well plate was determined using a microplate reader at 485/535 nm. Quantification of Na–F dye flux across the blank culture insert was also performed and transendothelial permeability coefficients (Pe) were measured for coculture as well as monolayer models.[56,59]

In Vitro Transfection through BBB Model.

In vitro BBB model was transferred to each well of a 24-well plate seeded with primary neurons.[60] Liposome formulations encapsulating ApoE2 pDNA were introduced into the culture insert. The insert was taken out 8 h postincubation, and cells were incubated for 2 days. ApoE ELISA kit was used to measure ApoE2 protein expression in cell lysates and supernatant media. Total protein was also quantified to normalize ApoE2 transfection.

Animal Procedures.

All live animal procedures were done in agreement with Institutional Animal Care and Use Committee (IACUC) approved protocol (#A17078). Six C57BL/6 mice (Jackson Laboratory, Bar Harbor, ME, USA) were used per group (3 males and 3 females). Animals were provided with adequate water and food.

Biocompatibility Evaluation and Gene Transfection in Wild-type Mice.

Liposome formulations (~15.2 nmol phospholipids/g body weight) entrapping pApoE2 (i.e., 1 μg pApoE2/g body weight) were injected intravenously in mice.[47] Various tissues (heart, spleen, liver, lungs, brain, and kidney) were collected on the sixth day of transfection, and histological assessment was done to determine *in vivo* biocompatibility. Briefly, formalin fixed tissue sections were embedded in paraffin, and hematoxylin–eosin (H&E) staining was performed.[61] Tissues were then examined for any abnormalities in morphology, infiltration of inflammatory cells, or necrosis. Transfection efficiency was also evaluated on the sixth day in all tissue samples and blood. Homogenization of tissue samples was performed utilizing phosphatase and protease inhibitor containing RIPA lysis buffer to prevent protein degradation. The resulting homogenate was centrifuged for 15 min at 4000 rpm to remove cell debris at 4 °C, and ApoE2 protein was quantified in the supernatant using ELISA.

Statistical Analysis.

Data is denoted as mean ± standard deviation (SD). The statistical analysis was done using *t* test or Tukey's test following one-way ANOVA. A *p*-value of 0.5 or below is considered to be statistically significant.

RESULTS AND DISCUSSION

AD affects the lives of millions of people worldwide. ApoE2 has been shown to enhance neuroprotection via multiple molecular mechanisms against AD.[15,21,62] However, the efficacy of systemically delivered ApoE2 protein is limited owing to its poor penetration across the BBB and short systemic half-life. Thus, *in situ* expression of the ApoE2 gene in brain tissue could be a feasible approach to treat AD. Nevertheless, gene therapy for brain disorders is challenging because of the absence of nontoxic and effectual gene delivery vectors that can evade the impeccable BBB. In this report, liposomal delivery systems dual-functionalized with a brain-specific ligand and CPP were developed not only to enhance their delivery across the BBB but improve internalization and expression of the therapeutic ApoE2 gene in the targeted brain cell as well.

Synthesis and Evaluation of Liposome Formulations.

Synthesis of CPP-conjugated PEGylated lipids is the foremost step in the development of dual-modified liposomes. The CPP conjugated lipid was prepared by reacting the *N*-hydroxysuccinimide ester of a PEGylated lipid with primary amines of the CPPs (RVG or Pen) under alkaline conditions. Micro-BCA protein assay was utilized to evaluate the extent of CPP conjugation to DSPE-PEG. In excess of 80% of the CPPs were able to successfully displace NHS from PEGylated lipid resulting in formation of CPP–lipid conjugates. The extent of RVG and Pen conjugation was found to be 82.64 ± 6.35%

and 81.94 ± 2.54%, respectively. Coating of PEG on the liposome surface prevents them from accretion, opsonization, and phagocytosis ensuring prolonged circulation time in the body.[63–65] Moreover, hydration cloud formation due to the presence of hydrophilic PEG chains around nanoparticles sterically hinders the contact between blood components and liposomes.[66] Thus, this restricts foreign material penetration into the PEG layer making it an efficient approach to prevent its clearance by macrophages.[67]

The CPP and MAN functionalized PEGylated liposomes were fabricated by a lipid film hydration approach. Size distribution by intensity of various liposome formulations is depicted in Figure 1A. The morphology of CPP and MAN conjugated liposomes was observed to be spherical, as shown in AFM images, with size less than 200 nm (Figure 1B,C). Hydrodynamic diameter, obtained using the DLS technique, of these liposomal formulations was found to be in agreement with AFM with a net positive zeta potential (Table 1). The positive surface charge of these formulations is primarily attributed to the presence of cationic lipid DOTAP. Polydispersity index (PDI) for all formulations was found to be less than 0.3, which indicates high particle homogeneity with no signs of aggregation.[68] Lastly, more than 80% of pApoE2 was found to be associated without any influence on size or PDI (Table 1).

DNase Protection Assay.

Gene delivery vectors play a crucial role in the protection of its genetic cargo against nucleases and lysosomal enzymes, which is essential for efficient gene therapy. Therefore, liposome formulations were assessed for their ability to protect the encapsulated pApoE2 against DNase I enzyme. As depicted in Figure 2, lane B, DNase I enzyme was capable of degrading pApoE2 completely in the absence of chitosan or liposomes, whereas liposomal formulations (Figure 2, lanes C–F) were efficient in preventing degradation of the genetic payload from DNase I digestion. This evidently shows that our liposome formulations have the potential to protect the therapeutic gene in a biological system against nucleases.

In Vitro Cytotoxicity Assay.

Interaction of nanoparticles, particularly cationic nanoparticles, with cellular and extracellular environments can trigger various biological processes, which can be detrimental to biocompatibility and efficacy of the formulation.[69] Therefore, prepared liposomal formulations entrapping pApoE–chitosan complex were assessed for their biocompatibility in bEnd.3, primary neurons, and astrocytes. Cells were treated with increasing concentration of phospholipids, and their effect on viability was analyzed via MTT assay. The relative cell viability in all the cell lines decreased with increasing concentration of the phospholipid (Figure 3), which is in accordance with data published by other researchers.[70,71] Treatment with 100 nM of phospholipids demonstrated more than 80% relative cell viability irrespective of the cell lines. The toxic effect of these nanoparticles at higher concentrations can be attributed to their positive charge as highly cationic nanoparticles induce disturbance in cellular membranes leading to cell death.[72] Therefore, liposomes at a dose of 100 nM of phospholipid was used in further experiments.

Cellular Mechanism of Uptake and Competition Assay.

The efficiency of nanoparticles to enter cells is crucial for effective delivery of therapeutic gene to the nucleus. Depending on their physiochemical characteristics, nanoparticles are internalized through various endocytosis pathways.[28] Therefore, to elucidate the exact mechanism for internalization for liposomes, different chemical moieties were used as inhibitors for different endocytosis pathways. Incubation at cold temperature (4 °C) or with sodium azide was used to prevent all ATP-dependent internalization pathways. Amiloride was used to inhibit micropinocytosis, while colchicine was used to prevent caveolae-mediated endocytosis by disruption of microtubules. Chlorpromazine was used to prevent formation of clathrin vesicles. Incubation at cold temperature (4 °C) or with sodium azide demonstrated significant decrease in the internalization of all the liposome formulations (Figure 4A). This suggests that more than 50% of internalization is contributed through some energy-dependent pathway. Inhibition of macropinocytosis using amiloride also resulted in significant reduction in liposomal uptake (more than 15%). Colchicine pretreatment did not show any effect on liposomes modified using Pen and PenMAN, indicating no role of caveolae-mediated endocytosis in these two formulations. Chlorpromazine pretreatment did not show any substantial effect on cellular internalization of RVG and RVGMAN modified liposomes indicating no role of clathrin-mediated endocytosis in their internalization process. Internalization of plain liposomes and MAN-liposomes was significantly reduced by 20% or more in the presence of various inhibitors, indicating more than one pathway was involved in internalization process of these formulations.

Similarly, the presence of physiological sugars can also affect the internalization of these liposomes by competing for glut-1 transporters present on astrocytes and the luminal side of BBB. Therefore, cells were pretreated with physiological levels of glucose and mannose before liposomal treatment. Also, a majority of AD patients (>80%) suffer from type 2 diabetes or glucose imbalance; therefore internalization of liposomes was also assessed in the presence of diabetic concentrations of glucose and mannose.[73] As demonstrated in Figure 4B, various liposomal formulations did not exhibit significant differences in cellular uptake by bEnd.3 cells, except MAN-functionalized liposomes. Internalization of MAN-liposomes was reduced by ~10% in the presence of physiological concentrations and by ~15% in the presence of diabetic sugar concentrations. This indicates competition for glucose transporter between sugar molecules present in culture medium and the MAN ligand on the liposomal surface. This competition was overcome using dual-functionalization of the liposome surface due to the presence of an additional glut-1 independent pathway (i.e., CPP-mediated) of internalization, justifying the use of two ligands to target brain cells.

In Vitro Transfection Efficiency.

An ideal gene delivery vector should facilitate safe and efficient transfer of its genetic payload in targeted cells to induce expression of therapeutic protein at a desired concentration. Primary neurons, primary astrocytes, and bEnd.3 cells were used to evaluate the liposome transfection ability. RVGMAN and PenMAN liposomes demonstrated significantly ($p < 0.05$) greater protein expression than pApoE2 alone (Figure 5). Dual-modified liposomes also showed 1.5-fold greater ($p < 0.05$) protein expression than plain or

monofunctionalized liposomes as well as Lipofectamine. The dual-functionalized liposome-mediated enhanced protein expression can be attributed to their higher cellular uptake and endosomal rupturing ability, which leads to enhanced transfer of therapeutic gene to the nucleus of the cells.[51] Complexation of pApoE2 with chitosan in combination with these factors may have collectively shown beneficial effect in enhancing protein expression via dual-functionalized liposomes.

Development of BBB Model.

The *in vitro* BBB model has emerged as a powerful tool for the assessment of brain targeted formulations.[74] The BBB model was developed utilizing coculture of primary astrocytes and bEnd.3 cells. TEER value and Na–F dye permeability across the barrier layer were measured to monitor integrity of the model. As shown in Figure 6A, the TEER of BBB model using dual cell lines was found to be significantly higher than a monolayer model. The TEER of the dual layer model was found to be 175 ± 17 Ω cm^2, whereas for the monolayer model, it was 104 ± 22 Ω cm^2. The TEER values across the barrier are in the range of 150–200 Ω cm^2, which is in accordance with data observed by other researchers.[75,76] Since the introduction of TEER method in 1981, it is the most commonly method used for evaluating the functionality of the BBB.[77] The measurement of TEER values in rats has been reported to be ~5900 Ω cm^2, which was much higher than the currently available BBB models.[78] Although, attempts have been made to replicate these values using brain astrocytes and endothelial cells from human origin, it only yielded TEER values of 140 Ω cm^2.[76] On the other hand, primary cells from rodents were able to achieve TEER values up to 300 Ω cm^2.[79] The advantage of using bEnd.3 cells in the BBB model system is that they grow rapidly and are able to retain their phenotype after several passages, making them convenient for developing an efficient BBB model.[80] Moreover, several tight junction proteins are found to be present in bEnd.3 cells like claudin-1, -3, and -5, occludin, zonula occludens-1 and -2, etc., which are absent in human based endothelial cells.[81] The result for Na–F dye flux was in accordance with TEER data as indicated in Figure 6B. Permeability coefficient of Na–F across monolayer model (Pe = ~1.302×10^{-5} cm/s) was found to be more than 6 times lower compared to that in the dual layer model (Pe = ~2.08×10^{-6} cm/s), indicating the influence of astrocytes on the integrity of the barrier model.[82–84]

In Vitro Transfection through the BBB Model.

The desired therapeutic effect of liposomes is achieved with efficient and effective translocation through the BBB and transfection of brain cells. Thus, transfection potential of various formulations was studied in primary neurons cultured below the BBB model. As depicted in Figure 6C, RVGMAN and PenMAN liposomes showed 2-fold greater transfection efficiency than plain and monofunctionalized liposomes. PenMAN liposomes demonstrated ~1.1 ng of ApoE protein/μg of total protein whereas RVGMAN liposomes showed ~0.9 ng of ApoE protein/μg of total protein. Although PenMAN-liposomes resulted in slightly higher transfection than RVGMAN-liposomes, no statistical significance ($p > 0.05$) was observed. Higher transfection efficiency of these nanoparticles might be associated with their superior translocation through the BBB and to the nucleus of the neurons. These results support the influence of modification on liposomes' surface with MAN in combination with CPP to translocate therapeutic genes in AD patients.

Biocompatibility Evaluation and Gene Transfection in Wild-type Mice.

Transfection of brain cells following transport of gene delivery vector across the BBB is essential to obtain desired therapeutic effect. Therefore, transfection of pApoE2/chitosan complex loaded liposomes was carried out in C57BL/6 mice following single tail vein administration. The organs of the treated animals were harvested 5-days postinjection to evaluate transfection levels using ApoE ELISA kit. As demonstrated in Figure 7A, dual-modified liposomes were able to successfully transfect brain cells and resulted in ~2 times higher ApoE protein expression than the endogenous ApoE level. Furthermore, RVGMAN and PenMAN liposomes demonstrated higher protein expression ($p < 0.05$) in mouse brain in contrast to naked pApoE2 and plain monofunctionalized liposomes. Both RVGMAN and PenMAN showed transfection in the range of 36.47 ± 4.38 and 37.69 ± 3.89 ng of ApoE2/mg of protein, respectively. Naked pApoE2 did not show any significant difference from endogenous level, whereas transfection efficiency of plain or monofunctionalized liposomes was found to be ~1.25 times endogenous levels. RVGMAN and PenMAN liposomes mediated greater ApoE2 protein expression possibly because the dual functionalization may have contributed to their higher and more efficient transcytosis and gene transport to the nucleus of the cells. Dual modification might have also helped the liposomes to overcome the competition from the physiological sugars present in the body. Therefore, dual-functionalized liposomes can serve as a promising candidate for brain-targeted delivery of pApoE2 to treat AD.

Tissues from other organs also displayed elevated ApoE2 expression *in vivo* (Figure 7B–G), which can be attributed to the transport of liposomes to these organs. The uptake of liposomes by reticuloendothelial system (RES) leads to their deposition in clearance organs.[85] Additionally, fenestration in the endothelial cells of capillaries enhances the trapping of liposomes justifying nonspecific distribution to these organs.[86]

Safety profiles of these nanoparticles were also assessed by the histopathological analysis of various tissues and compared against saline control. As depicted in Figure 8, no signs of abnormalities in morphology, infiltration of inflammatory cells, or necrosis in any organ tissue was found. Brain tissues of the treated mice appeared normal without any irregularly shaped nuclei or any other abnormalities. Similarly, liver tissue was devoid of any indication of ballooning or inflammation of hepatocytes. Examination of cardiac tissue depicted no signs of muscle fiber disruptions or myofibrillar loss. Similarly, signs of pulmonary fibrosis were not detected in lungs. These results indicate safety of liposome formulations suggesting a highly promising strategy to rescue AD patients from neurodegeneration and provide an assuring alternative to the current symptomatic therapy.

CONCLUSION

RVGMAN and PenMAN liposomes encapsulating ApoE2/chitosan complex significantly improved transport and transfection of ApoE2 gene across the *in vitro* BBB model. In addition, dual-functionalized liposomes were able to prevent the encapsulated gene from endonuclease digestion. Although gene delivery to brain is paved with numerous challenges, dual-functionalized liposomes were effective in brain-targeting and expression of genetic cargo in brain cells. This resulted in significantly increased levels of ApoE expression

in C57BL/6 mouse brain compared to other formulation controls. Furthermore, these formulations were found to be biocompatible as suggested by the absence of cell death or infiltration of inflammatory cells in tissues collected from treated animals. This indicates the potential of dual-functionalized liposomes as an effective gene delivery vector for the treatment of AD. Future studies will be performed in APP/PS1 transgenic mouse model to assess therapeutic efficacy of the optimized formulation to minimize amyloid beta protein levels in the brain.

Supplementary Material

Refer to Web version on PubMed Central for supplementary material.

ACKNOWLEDGMENTS

This research was supported by National Institutes of Health Grant R01AG051574.

REFERENCES

(1). Alzheimer's Association. 2018 Alzheimer's Disease Facts and Figures. Alzheimer's Dementia 2018, 14 (3), 367–342.

(2). Cummings JL; Morstorf T; Zhong K Alzheimer's Disease Drug-Development Pipeline: Few Candidates, Frequent Failures. Alzheimer's Res. Ther. 2014, 6 (4), 37. [PubMed: 25024750]

(3). Hurtado-Puerto AM; Russo C; Fregni F Alzheimer's Disease. Neuromethods 2018, 138, 297–338.

(4). Huang Y; Mucke L Alzheimer Mechanisms and Therapeutic Strategies. Cell 2012, 148 (6), 1204–1222. [PubMed: 22424230]

(5). Loera-Valencia R; Piras A; Ismail MAM; Manchanda S; Eyjolfsdottir H; Saido TC; Johansson J; Eriksdotter M; Winblad B; Nilsson P Targeting Alzheimer's Disease with Gene and Cell Therapies. J. Intern. Med. 2018, 284 (1), 2–36. [PubMed: 29582495]

(6). Liu C-C; Kanekiyo T; Xu H; Bu G Apolipoprotein E and Alzheimer Disease: Risk, Mechanisms and Therapy. Nat. Rev. Neurol. 2013, 9 (2), 106–118. [PubMed: 23296339]

(7). Ellis RJ; Olichney JM; Thal LJ; Mirra SS; Morris JC; Beekly D; Heyman A Cerebral Amyloid Angiopathy in the Brains of Patients with Alzheimer's Disease: The CERAD Experience, Part XV. Neurology 1996, 46 (6), 1592–1596. [PubMed: 8649554]

(8). Kok E; Haikonen S; Luoto T; Huhtala H; Goebeler S; Haapasalo H; Karhunen PJ Apolipoprotein E-Dependent Accumulation of Alzheimer Disease-Related Lesions Begins in Middle Age. Ann. Neurol. 2009, 65 (6), 650–657. [PubMed: 19557866]

(9). Verghese PB; Castellano JM; Holtzman DM Apolipoprotein E in Alzheimer's Disease and Other Neurological Disorders. Lancet Neurol. 2011, 10 (3), 241–252. [PubMed: 21349439]

(10). Mahley RW Apolipoprotein E: Remarkable Protein Sheds Light on Cardiovascular and Neurological Diseases. Clin. Chem. 2017, 63 (1), 14–20. [PubMed: 28062606]

(11). Mahley RW; Weisgraber KH; Huang Y Apolipoprotein E4: A Causative Factor and Therapeutic Target in Neuropathology, Including Alzheimer's Disease. Proc. Natl. Acad. Sci. U. S. A. 2006, 103 (15), 5644–5651. [PubMed: 16567625]

(12). Saunders AM; Strittmatter WJ; Schmechel D; St. George-Hyslop PH.; Pericak-Vance MA; Joo SH; Rosi BL; Gusella JF; Crapper-Mac Lachlan DR; Alberts MJ; Hulette C; Crain B; Goldgaber D; Roses AD Association of Apolipoprotein E Allele E4 with Late-Onset Familial and Sporadic Alzheimer's Disease. Neurology 1993, 43 (8), 1467. [PubMed: 8350998]

(13). Genin E; Hannequin D; Wallon D; Sleegers K; Hiltunen M; Combarros O; Bullido MJ; Engelborghs S; De Deyn P; Berr C; Pasquier F; Dubois B; Tognoni G; Fiévet N; Brouwers N; Bettens K; Arosio B; Coto E; Del Zompo M; Mateo I; Epelbaum J; Frank-Garcia A; Helisalmi S; Porcellini E; Pilotto A; Forti P; Ferri R; Scarpini E; Siciliano G; Solfrizzi V; Sorbi S; Spalletta G; Valdivieso F; Vepsäläinen S; Alvarez V; Bosco P; Mancuso M; Panza F; Nacmias B; Bossu P;

Hanon O; Piccardi P; Annoni G; Seripa D; Galimberti D; Licastro F; Soininen H; Dartigues JF; Kamboh MI; Van Broeckhoven C; Lambert JC; Amouyel P; Campion D APOE and Alzheimer Disease: A Major Gene with Semi-Dominant Inheritance. Mol. Psychiatry 2011, 16 (9), 903–907. [PubMed: 21556001]

(14). Sando SB; Melquist S; Cannon A; Hutton ML; Sletvold O; Saltvedt I; White LR; Lydersen S; Aasly JO APOE E4 Lowers Age at Onset and Is a High Risk Factor for Alzheimer's Disease; A Case Control Study from Central Norway. BMC Neurol. 2008, 8, 9. [PubMed: 18416843]

(15). Conejero-Goldberg C; Gomar JJ; Bobes-Bascaran T; Hyde TM; Kleinman JE; Herman MM; Chen S; Davies P; Goldberg TE APOE2 Enhances Neuroprotection against Alzheimer's Disease through Multiple Molecular Mechanisms. Mol. Psychiatry 2014, 19, 1243–1250. [PubMed: 24492349]

(16). Nagy ZS; Esiri MM; Jobst KA; Johnston C; Litchfield S; Sim E; Smith AD Influence of the Apolipoprotein E Genotype on Amyloid Deposition and Neurofibrillary Tangle Formation in Alzheimer's Disease. Neuroscience 1995, 69 (3), 757–761. [PubMed: 8596645]

(17). Castellano JM; Kim J; Stewart FR; Jiang H; DeMattos RB; Patterson BW; Fagan AM; Morris JC; Mawuenyega KG; Cruchaga C; Goate AM; Bales KR; Paul SM; Bateman RJ; Holtzman DM Human ApoE Isoforms Differentially Regulate Brain Amyloid-β Peptide Clearance. Sci. Transl. Med. 2011, 3 (89), 89ra57.

(18). Deane R; Sagare A; Hamm K; Parisi M; Lane S; Finn MB; Holtzman DM; Zlokovic BV ApoE Isoform-Specific Disruption of Amyloid β Peptide Clearance from Mouse Brain. J. Clin. Invest. 2008, 118 (12), 4002–4013. [PubMed: 19033669]

(19). Aleshkov S; Abraham CR; Zannis VI Interaction of Nascent Apoe2, Apoe3, and Apoe4 Isoforms Expressed in Mammalian Cells with Amyloid Peptide β (1–40). Relevance to Alzheimer's Disease. Biochemistry 1997, 36 (34), 10571–10580. [PubMed: 9265639]

(20). Jiang Q; Lee CYD; Mandrekar S; Wilkinson B; Cramer P; Zelcer N; Mann K; Lamb B; Willson TM; Collins JL; Richardson JC; Smith JD; Comery TA; Riddell D; Holtzman DM; Tontonoz P; Landreth GE ApoE Promotes the Proteolytic Degradation of Aβ. Neuron 2008, 58 (5), 681–693. [PubMed: 18549781]

(21). Bour A; Grootendorst J; Vogel E; Kelche C; Dodart JC; Bales K; Moreau PH; Sullivan PM; Mathis C Middle-Aged Human ApoE4 Targeted-Replacement Mice Show Retention Deficits on a Wide Range of Spatial Memory Tasks. Behav. Brain Res. 2008, 193 (2), 174–182. [PubMed: 18572260]

(22). Jiang CH; Tsien JZ; Schultz PG; Hu Y The Effects of Aging on Gene Expression in the Hypothalamus and Cortex of Mice. Proc. Natl. Acad. Sci. U. S. A. 2001, 98 (4), 1930–1934. [PubMed: 11172053]

(23). Pardo J; Morel G; Astiz M; Schwerdt J; Leon M; Rodriguez S; Herenu C; Goya R Gene Therapy and Cell Reprogramming For the Aging Brain: Achievements and Promise. Curr. Gene Ther. 2014, 14 (1), 24–34. [PubMed: 24450294]

(24). Naldini L Gene Therapy Returns to Centre Stage. Nature 2015, 526, 351–360. [PubMed: 26469046]

(25). Collins M; Thrasher A Gene Therapy: Progress and Predictions. Proc. R. Soc. London, Ser. B 2015, 282 (1821), 20143003.

(26). Gardlík R; Pálffy R; Hodosy J; Lukács J; Turňa J; Celec P Vectors and Delivery Systems in Gene Therapy. Med. Sci. Monit. 2005, 11 (4), RA110–21. [PubMed: 15795707]

(27). Nayerossadat N; Ali P; Maedeh T Viral and Nonviral Delivery Systems for Gene Delivery. Adv. Biomed. Res. 2012, 1, 27. [PubMed: 23210086]

(28). dos Santos Rodrigues B; Arora S; Kanekiyo T; Singh J Efficient Neuronal Targeting and Transfection Using RVG and Transferrin-Conjugated Liposomes. Brain Res. 2020, 1734, 146738. [PubMed: 32081534]

(29). Sharma D; Singh J Synthesis and Characterization of Fatty Acid Grafted Chitosan Polymer and Their Nanomicelles for Nonviral Gene Delivery Applications. Bioconjugate Chem. 2017, 28 (11), 2772–2783.

(30). Sharma D; Arora S; dos Santos Rodrigues B; Lakkadwala S; Banerjee A; Singh J Chitosan-Based Systems for Gene Delivery - Functional Chitosan: Drug Delivery and Biomedical Applications. In Functional Chitosan; Jana S., Jana S., Eds.; Springer Singapore: Singapore, 2019; pp 229–267.

(31). dos Santos Rodrigues B; Lakkadwala S; Sharma D; Singh J Chitosan for Gene, DNA Vaccines, and Drug Delivery. Materials for Biomedical Engineering; Elsevier, 2019; pp 515–550.

(32). Umezawa F; Eto Y Liposome Targeting to Mouse Brain: Mannose as a Recognition Marker. Biochem. Biophys. Res. Commun. 1988, 153 (3), 1038–1044. [PubMed: 3390170]

(33). Tsuji A Small Molecular Drug Transfer across the Blood-Brain Barrier via Carrier-Mediated Transport Systems. NeuroRx 2005, 2 (1), 54–62. [PubMed: 15717057]

(34). Kim JY; Choi W. Il; Kim YH; Tae G. Brain-Targeted Delivery of Protein Using Chitosan- and RVG Peptide-Conjugated, Pluronic-Based Nano-Carrier. Biomaterials 2013, 34 (4), 1170–1178. [PubMed: 23122677]

(35). Liu Y; Guo Y; An S; Kuang Y; He X; Ma H; Li J; Lv J; Zhang N; Jiang C Targeting Caspase-3 as Dual Therapeutic Benefits by RNAi Facilitating Brain-Targeted Nanoparticles in a Rat Model of Parkinson's Disease. PLoS One 2013, 8 (5), No. e62905. [PubMed: 23675438]

(36). Koren E; Torchilin VP Cell-Penetrating Peptides: Breaking through to the Other Side. Trends Mol. Med. 2012, 18 (7), 385–393. [PubMed: 22682515]

(37). Jin G-Z; Chakraborty A; Lee J-H; Knowles JC; Kim H-W Targeting with Nanoparticles for the Therapeutic Treatment of Brain Diseases. J. Tissue Eng. 2020, 11, 204173141989746.

(38). Sun J; Xie W; Zhu X; Xu M; Liu J Sulfur Nanoparticles with Novel Morphologies Coupled with Brain-Targeting Peptides RVG as a New Type of Inhibitor Against Metal-Induced Aβ Aggregation. ACS Chem. Neurosci. 2018, 9 (4), 749–761. [PubMed: 29192759]

(39). Joo J; Kwon EJ; Kang J; Skalak M; Anglin EJ; Mann AP; Ruoslahti E; Bhatia SN; Sailor MJ Porous Silicon-Graphene Oxide Core-Shell Nanoparticles for Targeted Delivery of SiRNA to the Injured Brain. Nanoscale Horizons 2016, 1 (5), 407–414. [PubMed: 29732165]

(40). Arora S; Sharma D; Singh J GLUT-1: An Effective Target To Deliver Brain-Derived Neurotrophic Factor Gene Across the Blood Brain Barrier. ACS Chem. Neurosci. 2020, 11 (11), 1620–1633. [PubMed: 32352752]

(41). Lakkadwala S; dos Santos Rodrigues B; Sun C; Singh J Dual Functionalized Liposomes for Efficient Co-Delivery of Anti-Cancer Chemotherapeutics for the Treatment of Glioblastoma. J. Controlled Release 2019, 307, 247–260.

(42). Škrlj N; Drevenšek G; Hudoklin S; Romih R; Čurin Šerbec V; Dolinar M Recombinant Single-Chain Antibody with the Trojan Peptide Penetratin Positioned in the Linker Region Enables Cargo Transfer across the Blood-Brain Barrier. Appl. Biochem. Biotechnol. 2013, 169 (1), 159–169. [PubMed: 23160949]

(43). Xia H; Gao X; Gu G; Liu Z; Hu Q; Tu Y; Song Q; Yao L; Pang Z; Jiang X; Chen J; Chen H Penetratin-Functionalized PEG-PLA Nanoparticles for Brain Drug Delivery. Int. J. Pharm. 2012, 436 (1–2), 840–850. [PubMed: 22841849]

(44). Sarko D; Beijer B; Garcia Boy R; Nothelfer EM; Leotta K; Eisenhut M; Altmann A; Haberkorn U; Mier W The Pharmacokinetics of Cell-Penetrating Peptides. Mol. Pharmaceutics 2010, 7 (6), 2224–2231.

(45). Zhao N; Liu CC; Qiao W; Bu G Apolipoprotein E, Receptors, and Modulation of Alzheimer's Disease. Biol. Psychiatry 2018, 83 (4), 347–357. [PubMed: 28434655]

(46). Matsumoto T; Rauskolb S; Polack M; Klose J; Kolbeck R; Korte M; Barde YA Biosynthesis and Processing of Endogenous BDNF: CNS Neurons Store and Secrete BDNF, Not pro-BDNF. Nat. Neurosci. 2008, 11 (2), 131–133. [PubMed: 18204444]

(47). dos Santos Rodrigues B; Kanekiyo T; Singh J ApoE-2 Brain-Targeted Gene Therapy Through Transferrin and Penetratin Tagged Liposomal Nanoparticles. Pharm. Res. 2019, 36 (11), 161. [PubMed: 31529284]

(48). Zhang HW; Zhang L; Sun X; Zhang ZR Successful Transfection of Hepatoma Cells after Encapsulation of Plasmid DNA into Negatively Charged Liposomes. Biotechnol. Bioeng. 2007, 96 (1), 118–124. [PubMed: 16894635]

(49). Sumners C; Fregly MJ Modulation of Angiotensin II Binding Sites in Neuronal Cultures by Mineralocorticoids. Am. J. Physiol. - Cell Physiol. 1989, 256 (1), C121–C129.

(50). dos Santos Rodrigues B; Oue H; Banerjee A; Kanekiyo T; Singh J Dual Functionalized Liposome-Mediated Gene Delivery across Triple Co-Culture Blood Brain Barrier Model and Specific in Vivo Neuronal Transfection. J. Controlled Release 2018, 286, 264–278.

(51). dos Santos Rodrigues B; Banerjee A; Kanekiyo T; Singh J Functionalized Liposomal Nanoparticles for Efficient Gene Delivery System to Neuronal Cell Transfection. Int. J. Pharm. 2019, 566, 717–730. [PubMed: 31202901]

(52). Sharma D; Arora S; Singh J Smart Thermosensitive Copolymer Incorporating Chitosan-Zinc-Insulin Electrostatic Complexes for Controlled Delivery of Insulin: Effect of Chitosan Chain Length. Int. J. Polym. Mater. 2019, 1–15.

(53). Lipp L; Sharma D; Banerjee A; Singh J Controlled Delivery of Salmon Calcitonin Using Thermosensitive Triblock Copolymer Depot for Treatment of Osteoporosis. ACS Omega 2019, 4 (1), 1157–1166. [PubMed: 30729223]

(54). Layek B; Haldar MK; Sharma G; Lipp L; Mallik S; Singh J Hexanoic Acid and Polyethylene Glycol Double Grafted Amphiphilic Chitosan for Enhanced Gene Delivery: Influence of Hydrophobic and Hydrophilic Substitution Degree. Mol. Pharmaceutics 2014, 11 (3), 982–994.

(55). Sharma G; Lakkadwala S; Modgil A; Singh J The Role of Cell-Penetrating Peptide and Transferrin on Enhanced Delivery of Drug to Brain. Int. J. Mol. Sci. 2016, 17 (6), 806. [PubMed: 27231900]

(56). Sharma G; Modgil A; Sun C; Singh J Grafting of Cell-Penetrating Peptide to Receptor-Targeted Liposomes Improves Their Transfection Efficiency and Transport across Blood-Brain Barrier Model. J. Pharm. Sci. 2012, 101 (7), 2468–2478. [PubMed: 22517732]

(57). Ying X; Wen H; Lu WL; Du J; Guo J; Tian W; Men Y; Zhang Y; Li RJ; Yang TY; Shang DW; Lou JN; Zhang LR; Zhang Q Dual-Targeting Daunorubicin Liposomes Improve the Therapeutic Efficacy of Brain Glioma in Animals. J. Controlled Release 2010, 141 (2), 183–192.

(58). Nakagawa S; Deli MA; Kawaguchi H; Shimizudani T; Shimono T; Kittel Á; Tanaka K; Niwa M A New Blood-Brain Barrier Model Using Primary Rat Brain Endothelial Cells, Pericytes and Astrocytes. Neurochem. Int. 2009, 54 (3–4), 253–263. [PubMed: 19111869]

(59). Veszelka S; Pásztói M; Farkas AE; Krizbai I; Dung NTK; Niwa M; Ábrahám CS; Deli MA Pentosan Polysulfate Protects Brain Endothelial Cells against Bacterial Lipopolysaccharide-Induced Damages. Neurochem. Int. 2007, 50 (1), 219–228. [PubMed: 16997427]

(60). dos Santos Rodrigues B; Lakkadwala S; Kanekiyo T; Singh J Development and Screening of Brain-Targeted Lipid-Based Nanoparticles with Enhanced Cell Penetration and Gene Delivery Properties. Int. J. Nanomed. 2019, 14, 6497–6517.

(61). Sharma D; Singh J Long-Term Glycemic Control and Prevention of Diabetes Complications in Vivo Using Oleic Acid-Grafted-Chitosan-zinc-Insulin Complexes Incorporated in Thermosensitive Copolymer. J. Controlled Release 2020, 323, 161–178.

(62). Rodriguez GA; Burns MP; Weeber EJ; Rebeck GW Young APOE4 Targeted Replacement Mice Exhibit Poor Spatial Learning and Memory, with Reduced Dendritic Spine Density in the Medial Entorhinal Cortex. Learn. Mem. 2013, 20 (5), 256–266. [PubMed: 23592036]

(63). Suk JS; Xu Q; Kim N; Hanes J; Ensign LM PEGylation as a Strategy for Improving Nanoparticle-Based Drug and Gene Delivery. Adv. Drug Delivery Rev. 2016, 99, 28–51.

(64). Klibanov AL; Maruyama K; Torchilin VP; Huang L Amphipathic Polyethyleneglycols Effectively Prolong the Circulation Time of Liposomes. FEBS Lett. 1990, 268 (1), 235–237. [PubMed: 2384160]

(65). Kim J; Kim PH; Kim SW; Yun CO Enhancing the Therapeutic Efficacy of Adenovirus in Combination with Biomaterials. Biomaterials 2012, 33 (6), 1838–1850. [PubMed: 22142769]

(66). Yang Q; Lai SK Anti-PEG Immunity: Emergence, Characteristics, and Unaddressed Questions. Wiley Interdiscip. Rev. Nanomedicine Nanobiotechnology 2015, 7 (5), 655–677. [PubMed: 25707913]

(67). Vonarbourg A; Passirani C; Saulnier P; Benoit JP Parameters Influencing the Stealthiness of Colloidal Drug Delivery Systems. Biomaterials 2006, 27 (24), 4356–4373. [PubMed: 16650890]

(68). Danaei M; Dehghankhold M; Ataei S; Hasanzadeh Davarani F; Javanmard R; Dokhani A; Khorasani S; Mozafari MR Impact of Particle Size and Polydispersity Index on the Clinical Applications of Lipidic Nanocarrier Systems. Pharmaceutics 2018, 10, 57. [PubMed: 29783687]

(69). Naahidi S; Jafari M; Edalat F; Raymond K; Khademhosseini A; Chen P Biocompatibility of Engineered Nanoparticles for Drug Delivery. J. Controlled Release 2013, 166 (2), 182–194.

(70). Rosada RS; Torre L; Frantz FG; Trombone APF; Zárate-Bladés CR; Fonseca DM; Souza PRM; Brandão IT; Masson AP; Soares ÉG; Ramos SG; Faccioli LH; Silva CL; Santana MHA; Coelho-Castelo AAM Protection against Tuberculosis by a Single Intranasal Administration of DNA-Hsp65 Vaccine Complexed with Cationic Liposomes. BMC Immunol. 2008, 9, 38. [PubMed: 18647414]

(71). Lechanteur A; Sanna V; Duchemin A; Evrard B; Mottet D; Piel G Cationic Liposomes Carrying SiRNA: Impact of Lipid Composition on Physicochemical Properties, Cytotoxicity and Endosomal Escape. Nanomaterials 2018, 8 (5), 270. [PubMed: 29695068]

(72). Fröhlich E The Role of Surface Charge in Cellular Uptake and Cytotoxicity of Medical Nanoparticles. Int. J. Nanomed. 2012, 7, 5577–5591.

(73). Janson J; Laedtke T; Parisi JE; O'Brien P; Petersen RC; Butler PC Increased Risk of Type 2 Diabetes in Alzheimer Disease. Diabetes 2004, 53 (2), 474–481. [PubMed: 14747300]

(74). Helms HC; Abbott NJ; Burek M; Cecchelli R; Couraud PO; Deli MA; Förster C; Galla HJ; Romero IA; Shusta EV; Stebbins MJ; Vandenhaute E; Weksler B; Brodin B In Vitro Models of the Blood-Brain Barrier: An Overview of Commonly Used Brain Endothelial Cell Culture Models and Guidelines for Their Use. J. Cereb. Blood Flow Metab. 2016, 36 (5), 862–890. [PubMed: 26868179]

(75). Booth R; Kim H Characterization of a Microfluidic in Vitro Model of the Blood-Brain Barrier (MBBB). Lab Chip 2012, 12 (10), 1784–1792. [PubMed: 22422217]

(76). Daniels BP; Cruz-Orengo L; Pasieka TJ; Couraud PO; Romero IA; Weksler B; Cooper JA; Doering TL; Klein RS Immortalized Human Cerebral Microvascular Endothelial Cells Maintain the Properties of Primary Cells in an in Vitro Model of Immune Migration across the Blood Brain Barrier. J. Neurosci. Methods 2013, 212 (1), 173–179. [PubMed: 23068604]

(77). Crone C; Olesen SP Electrical Resistance of Brain Microvascular Endothelium. Brain Res. 1982, 241 (1), 49–55. [PubMed: 6980688]

(78). Butt AM; Jones HC; Abbott NJ Electrical Resistance across the Blood-brain Barrier in Anaesthetized Rats: A Developmental Study. J. Physiol. 1990, 429 (1), 47–62. [PubMed: 2277354]

(79). Abbott NJ; Dolman DEM; Drndarski S; Fredriksson SM An Improved in Vitro Blood-Brain Barrier Model: Rat Brain Endothelial Cells Co-Cultured with Astrocytes. Methods Mol. Biol. 2012, 814, 415–430. [PubMed: 22144323]

(80). Brown RC; Morris AP; O'Neil RG Tight Junction Protein Expression and Barrier Properties of Immortalized Mouse Brain Microvessel Endothelial Cells. Brain Res. 2007, 1130 (1), 17–30. [PubMed: 17169347]

(81). Rahman NA; Rasil ANHM; Meyding-Lamade U; Craemer EM; Diah S; Tuah AA; Muharram SH Immortalized Endothelial Cell Lines for in Vitro Blood-Brain Barrier Models: A Systematic Review. Brain Res. 2016, 1642, 532–545. [PubMed: 27086967]

(82). Sharma G; Modgil A; Zhong T; Sun C; Singh J Influence of Short-Chain Cell-Penetrating Peptides on Transport of Doxorubicin Encapsulating Receptor-Targeted Liposomes across Brain Endothelial Barrier. Pharm. Res. 2014, 31 (5), 1194–1209. [PubMed: 24242938]

(83). Janzer RC; Raff MC Astrocytes Induce Blood-Brain Barrier Properties in Endothelial Cells. Nature 1987, 325 (6101), 253–257. [PubMed: 3543687]

(84). Arthur FE; Shivers RR; Bowman PD Astrocyte-Mediated Induction of Tight Junctions in Brain Capillary Endothelium: An Efficient in Vitro Model. Dev. Brain Res. 1987, 36 (1), 155–159.

(85). Li SD; Huang L Nanoparticles Evading the Reticuloendothelial System: Role of the Supported Bilayer. Biochim. Biophys. Acta, Biomembr. 2009, 1788 (10), 2259–2266.

(86). Haute DV; Berlin JM Challenges in Realizing Selectivity for Nanoparticle Biodistribution and Clearance: Lessons from Gold Nanoparticles. Ther. Delivery 2017, 8 (9), 763–774.

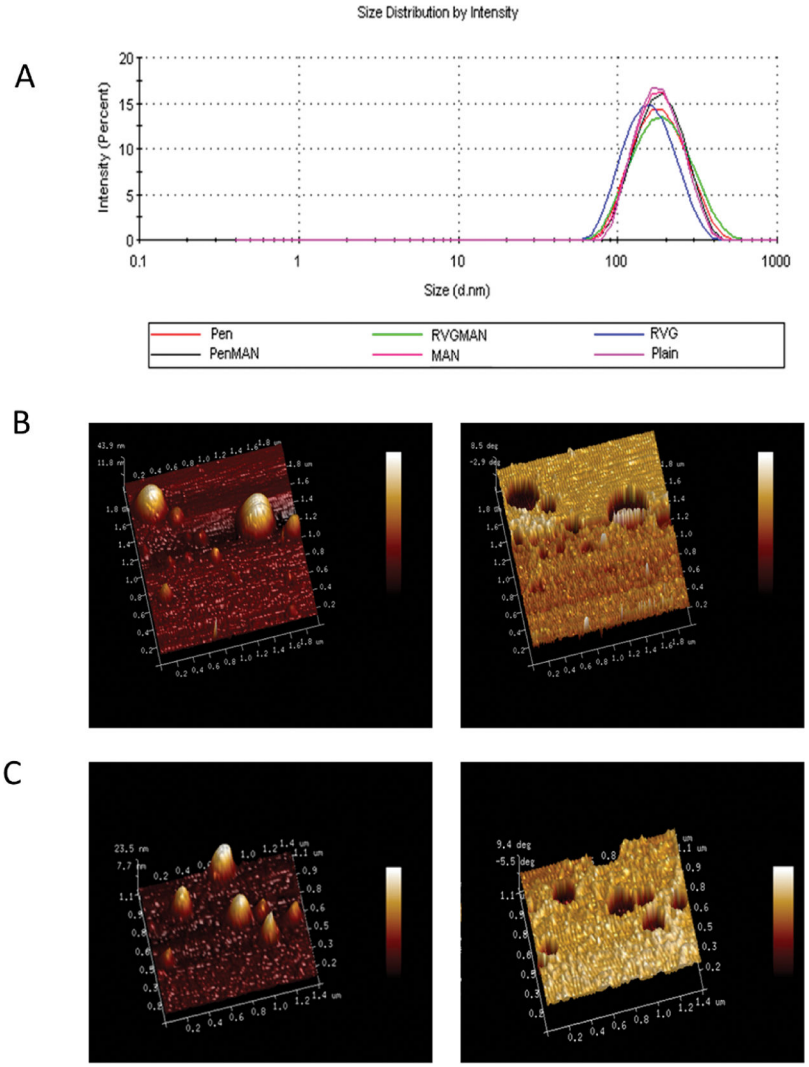

Figure 1.

(A) Distribution of particle size for different liposome formulations using DLS method. AFM images (normal and phase contrast) of (B) PenMAN and (C) RVGMAN liposomes.

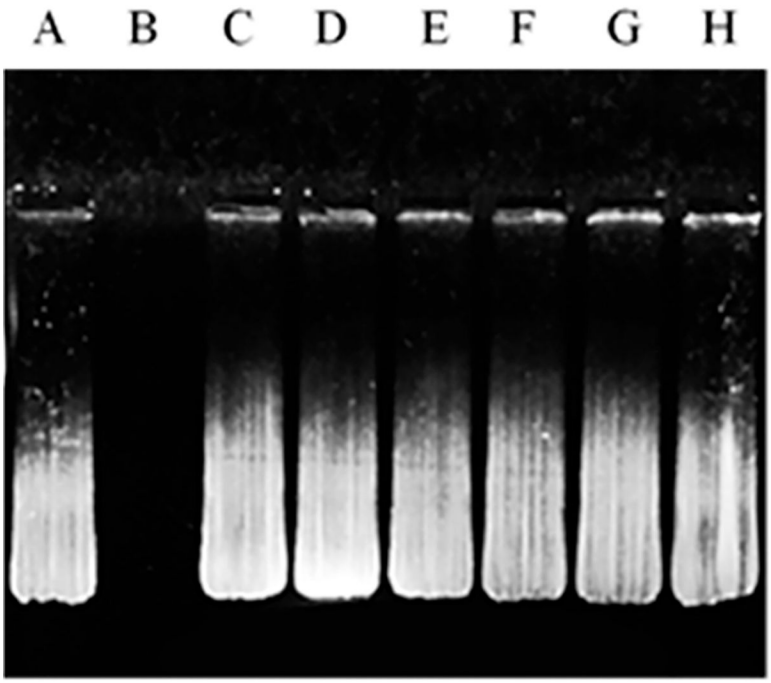

Figure 2.

DNase I protection assay. Liposomes containing chitosan/pApoE2 complex was incubated with DNase I enzyme. Lane A, naked pApoE2; lane B, pApoE2 + DNase I; lanes C–H, pApoE2/chitosan complexes loaded in plain, MAN, Pen, PenMAN, RVG, or RVGMAN liposomes, respectively, plus DNase I.

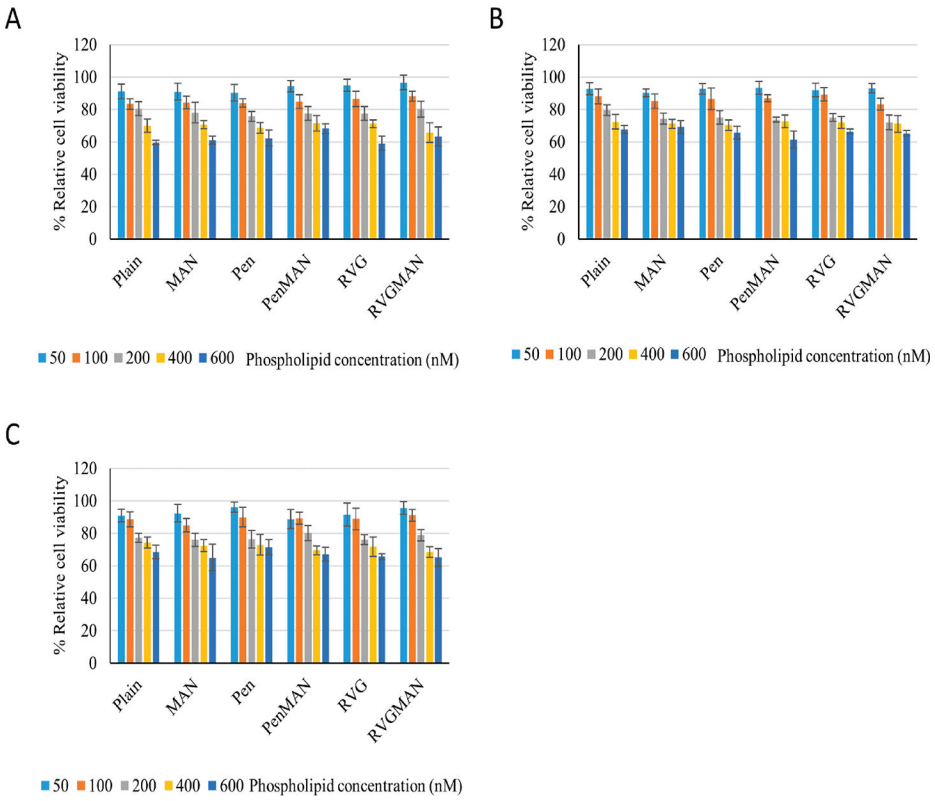

Figure 3.

In vitro cytocompatibility of liposomes at various phospholipid concentrations on (A) bEnd.3, (B) primary astrocytes, and (C) primary neurons. Data represent mean ± SD of four replicates.

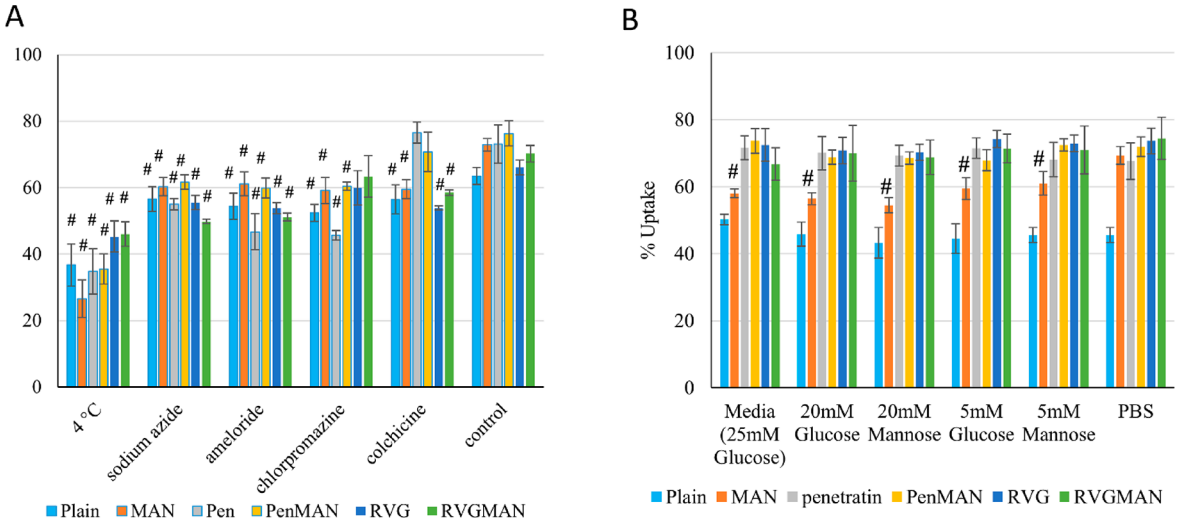

Figure 4.

Quantitative analysis of (A) cellular uptake mechanism and (B) competition assay in bEnd.3 cells. Data represent mean ± SD of four replicates. # indicates statistically ($p < 0.05$) different from their respective PBS control.

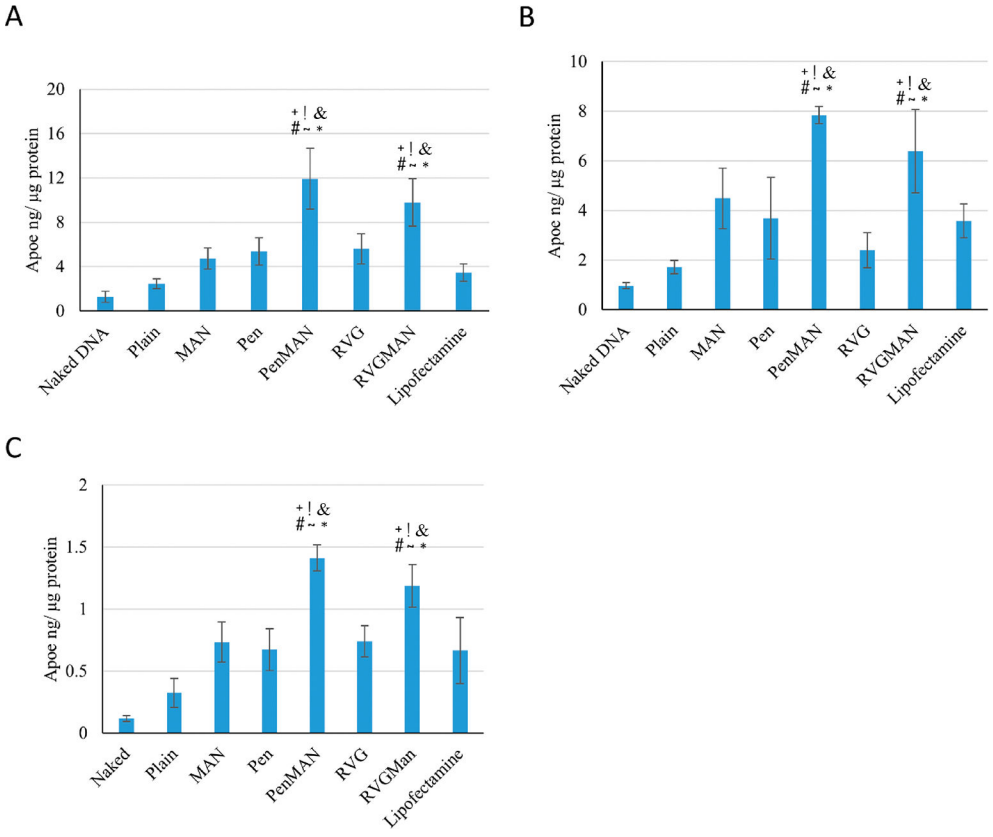

Figure 5.

Transfection of ApoE2 in (A) bEnd.3 cells, (B) primary astrocytes, and (C) primary neurons using various chitosan/pApoE2 (1 µg) loaded liposomes. Data represent mean ± SD of four replicates. *, #, +, &, !, and ~ indicate statistically ($p < 0.05$) different from plain, MAN, Pen, RVG liposomes, naked DNA, and lipofectamine, respectively.

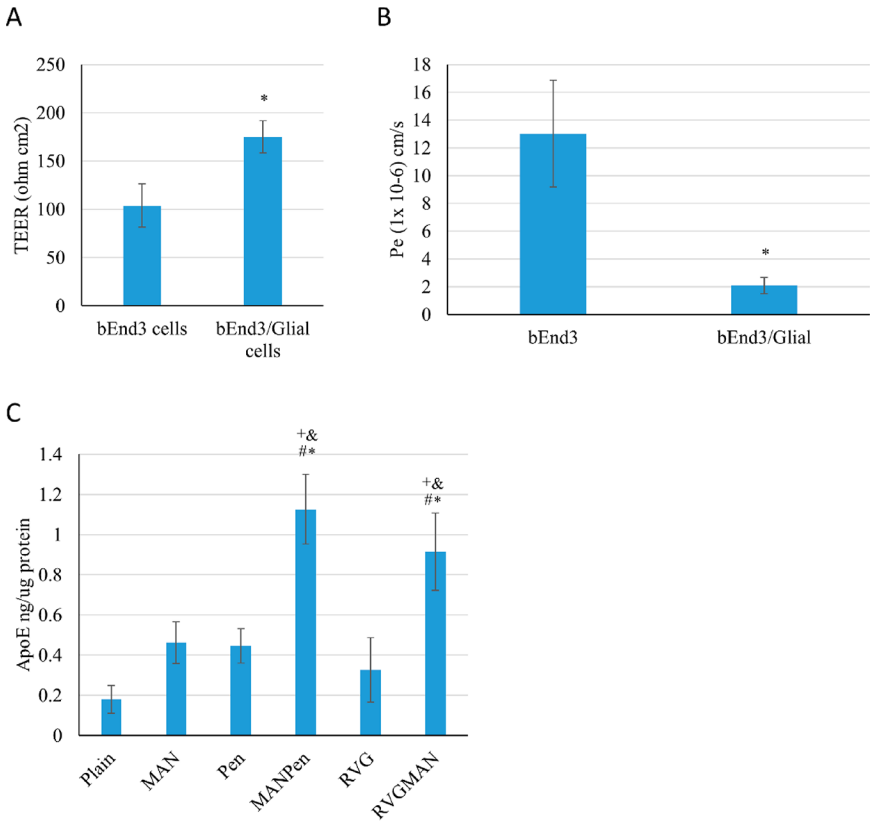

Figure 6.

In vitro BBB model. (A) TEER value and (B) Na–F permeability coefficient. Data represent mean ± SD of four replicates (*$p < 0.05$). (C) ApoE2 protein expression in primary neurons. Data represent mean ± SD of four replicates. *, #, +, and & indicate statistically ($p < 0.05$) different from plain, MAN, Pen, and RVG liposomes, respectively.

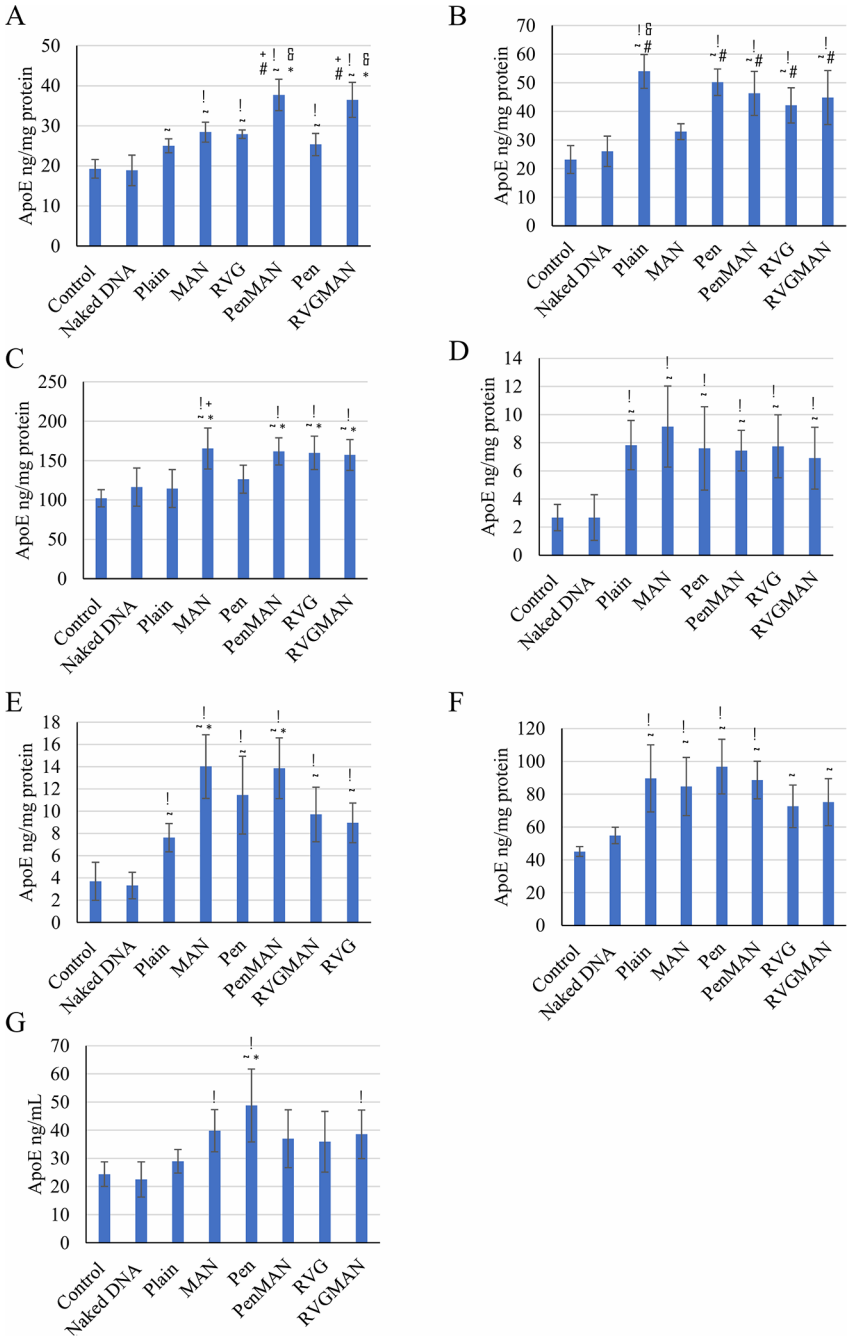

Figure 7.

ApoE concentration in various mouse tissues ((A) brain; (B) heart; (C) liver; (D) spleen; (E) lungs; (F) kidney; (G) plasma) following tail vein administration of pApoE2/chitosan loaded liposomes (15.2 nM of total lipids containing 1 μg pApoE2/g body weight). Data represent mean ± SD of four replicates. *, #, +, &, !, and ~ indicate statistically ($p < 0.05$) different from plain, MAN, Pen, RVG liposomes, naked DNA, and control, respectively.

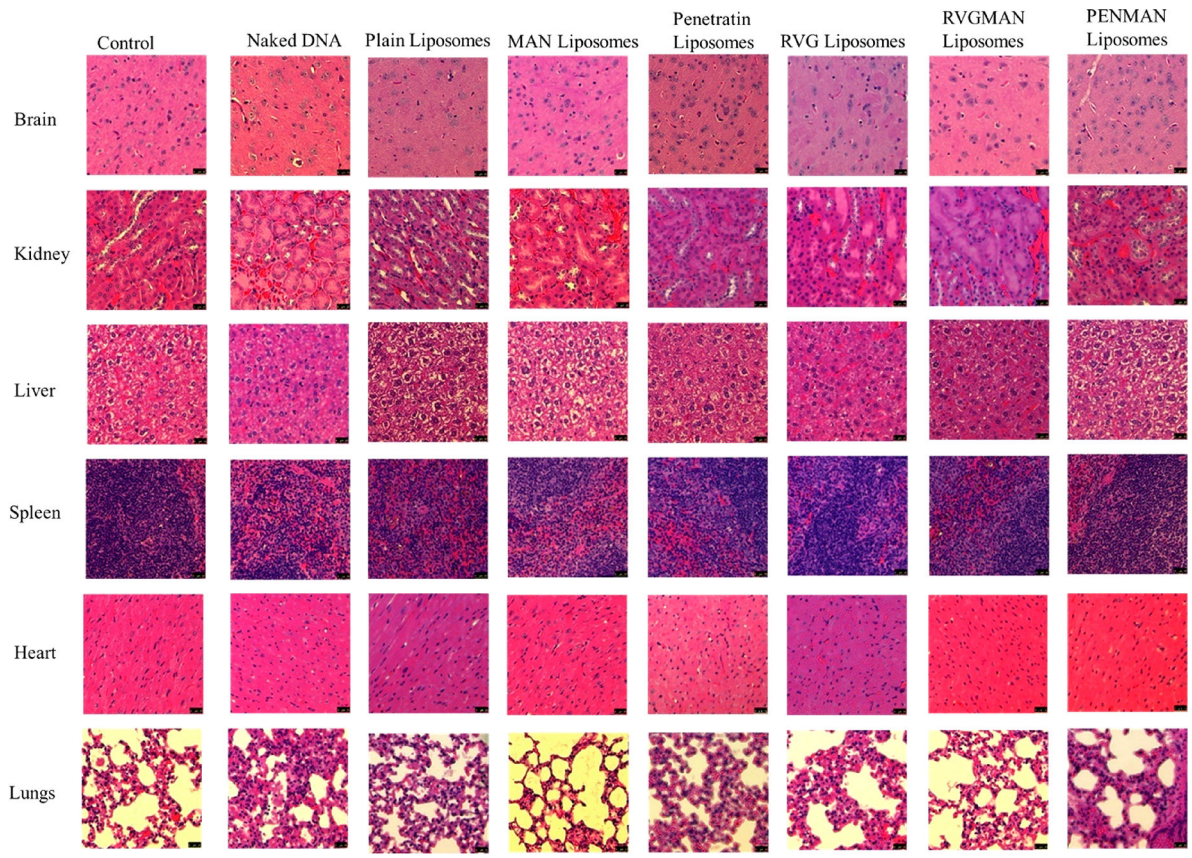

Figure 8.

Biocompatibility assessment of different liposomal formulations following H&E staining post-ApoE2 transfection in different organs.

Table 1.

Characterization of pApoE2 Entrapped Liposomes[a]

formulation	particle size (nm)	zeta potential (mV)	PDI	entrapment efficiency (%)
plain liposomes	178.6 ± 0.90	16.4 ± 0.5	0.302 ± 0.18	86.78 ± 1.62
MAN liposomes	160.9 ± 7.44 *	14.9 ± 5.8	0.238 ± 0.12	83.79 ± 4.44
Pen liposomes	171.5 ± 4.91 #	19.9 ± 1.3	0.230 ± 0.09	88.40 ± 6.20
PenMAN liposomes	172.0 ± 3.09 #^	19.0 ± 0.9	0.191 ± 0.04	86.30 ± 1.55
RVG liposomes	154.6 ± 3.96 *+	18.5 ± 0.1	0.249 ± 0.01	85.50 ± 2.25
RVGMAN liposomes	167.8 ± 2.47 *^	19.8 ± 3.6	0.132 ± 0.10	84.50 ± 5.90

[a]Data represent mean ± SD of four replicates.

*, #, +, and ^ indicate statistically ($p < 0.05$) different from plain, MAN, Pen, and RVG liposomes, respectively.